Surface Modification of Ceramic Nanoparticles via Atomic Layer Deposition

Luis F. Hakim [a], Steven M. George [a,b], Alan W. Weimer [a, *]
[a] *Department of Chemical and Biological Engineering, University of Colorado, Boulder, CO 80309, USA*
[b] *Department of Chemistry and Biochemistry, University of Colorado, Boulder, CO 80309, USA*

Keywords: Atomic Layer Deposition, nanoparticles, fluidization, conformal coating, ultrathin films

Abstract
Silica nanoparticles (40 nm) were individually and conformally coated with alumina films using Atomic Layer Deposition (ALD) in a fluidized bed reactor. Films were deposited using self-limiting sequential surface reactions of trimethylaluminum and water. Alumina vibrational modes were observed using Transmission Infrared Spectroscopy. X-ray Photoelectron Spectroscopy indicated complete coverage on the surface as the silica features were completely attenuated. Scanning Electron Microscopy and Energy Dispersive Spectroscopy showed high uniformity of the deposited films. Transmission Electron Microscopy revealed extremely conformal films with an average growth rate of 0.11 nm/cycle. Self-limiting characteristics of ALD allowed primary nanoparticles to be coated as they fluidized as dynamic aggregates.

1. Introduction
Composites of aluminum-based compounds and fumed silica particles are commonly used as fillers to improve the wear resistance of dental restorative materials [1]. Controlling the optical properties of these fillers, such as the refractive index, is desirable [2]. For fillers composed of fumed silica particles coated with a thin film, this control involves precisely varying the thickness of the thin film. A novel technology based on the use of Atomic Layer Deposition (ALD) in a fluidized bed reactor is proposed as a method to deposit conformal and uniform films on the surface of individual nanoparticles.

Depositing ultrathin films on primary nanoparticles using methods such as wet chemical processing and chemical vapor deposition (CVD) is difficult [3]. During a CVD reaction, the chemical reactants are allowed to coexist in the gas phase where competing homogeneous reactions form nanoparticles that are ultimately scavenged on the substrate particles. A CVD reaction occurs continuously with no self-control and is dependent upon reaction time, reactant exposure, pressure and temperature [4, 5]. Various CVD technologies have been successfully applied to particles [6-11]. However, truly uniform and conformal films on individual nanoparticles have not been achieved mainly due to particle aggregation.

Atomic Layer Deposition (ALD) is independent of line of sight and provides an ideal method for depositing ultrathin films on high aspect ratio surfaces [12-14]. ALD uses sequential surface chemical reactions to deposit films with high conformality and exact control at the atomic scale. ALD precursors react only after they have been adsorbed on the particle

* Corresponding author. Tel +1-303-492-7471; fax: +1-303-492-4341
E-mail address: alan.weimer@colorado.edu (A.W. Weimer).

surface. Adsorption of gas phase reactants occurs only while there are active sites available on the substrate.

Deposition of alumina films using a progression of surface reactions has been demonstrated [15-20]. Trimethylaluminum [$Al(CH_3)_3$] (TMA) and water vapor are employed alternately in an ABAB… binary reaction sequence. Film deposition is based in the following binary CVD reaction:

$$2Al(CH_3)_3 + 3H_2O \rightarrow Al_2O_3 + 6CH_4 \quad (1)$$

Al_2O_3 ALD is achieved by splitting this reaction into two separate half-reactions [17]:

$$(A)\ 2AlOH^* + 2Al(CH_3)_3 \rightarrow 2[AlOAl(CH_3)_2]^* + 2CH_4 \quad (2)$$

$$(B)\ 2[AlOAl(CH_3)_2]^* + 3H_2O \rightarrow Al_2O_3 + 2AlOH^* + 4CH_4 \quad (3)$$

where the asterisks designate the surface species. After sequential exposures of $Al(CH_3)_3$ and H_2O at 450 K, the thickness of the film is approximately 0.11 nm per coating cycle [21].

Nanoparticles have been successfully coated with ultrathin films at small scale for several ALD systems [22]. Bulk quantities of metal and ceramic micron-sized particles have been coated with alumina using ALD in a fluidized bed reactor [23, 24].

As the use of nanoparticles increases, the need for large-scale bulk processing also increases. The present study is the first successful attempt to conformally coat individual fumed silica nanoparticles at large scale using ALD in a fluidized bed reactor.

2. Results

2.1 Fluidization and aggregation characteristics

Given that the ALD coating was performed in a fluidized bed reactor, understanding the fluidization of silica nanoparticles is a key step in perfecting the coating process. In general, due to high London-Van der Waals forces, nanoparticles fluidize as aggregates [25-27]. Aggregates of silica nanoparticles were observed during fluidization using a high-speed laser imaging system (Figure 1).

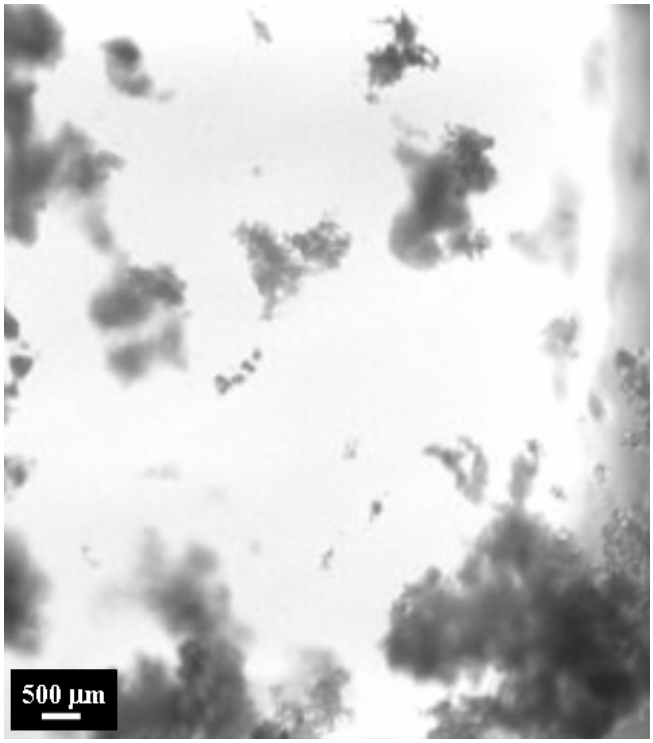

Figure 1. Fluidized aggregates of Aerosil OX-50^{TM} silica nanoparticles.

The images are collected in a region known as the splash zone of the fluidized bed. This region was selected for imaging because aggregates momentarily separate from the bed surface, thus allowing their visualization. This region was located below the disengagement zone, where elutriation levels are low, assuring that the size distribution of the aggregates was representative of the one in the bed. As determined using the laser imaging system, the fluidized aggregates are several hundreds of microns in size.

The properties of aggregates, rather than those of primary particles, will determine the fluidization properties of nanoparticles. Aggregate properties such as size, density, sphericity and surface roughness will dictate fluidization properties such as bed expansion and minimum fluidization velocity.

Due to constant solids recirculation and an excellent fluid-solid contacting, a fluidized bed offers great advantages over other reactor configurations. A fluidized bed shows high heat and mass transfer coefficients as well as a rapid solids mixing. In an ALD system, this characteristic would help achieve fast saturation of active sites on the particle surface. Therefore, a fluidized state must be assured at all times during processing. The minimum fluidization velocity of the silica nanoparticles used in this study is about 0.02 cm/s, determined by measuring the pressure drop across the bed versus the superficial gas velocity. This shows that silica nanoparticles fluidize smoothly despite their small size and high aggregation tendency and that a fluidized bed is very suitable for ALD processing.

2.2 Test for conformality, uniformity and composition of films

Transmission electron microscopy (TEM) was used to analyze the conformality of alumina films as well as to approximate their thickness. A micrograph of coated nanoparticles after 50 cycles is shown in Figure 2. From visual inspection, the growth rate is calculated to be in the range of 0.09-0.12 nm/cycle. The growth rate of the ALD films may vary with the size and geometry of the substrate. For high aspect ratio surfaces, less steric effects occur and more active sites are exposed to the gas precursors during the adsorption step of the reaction.

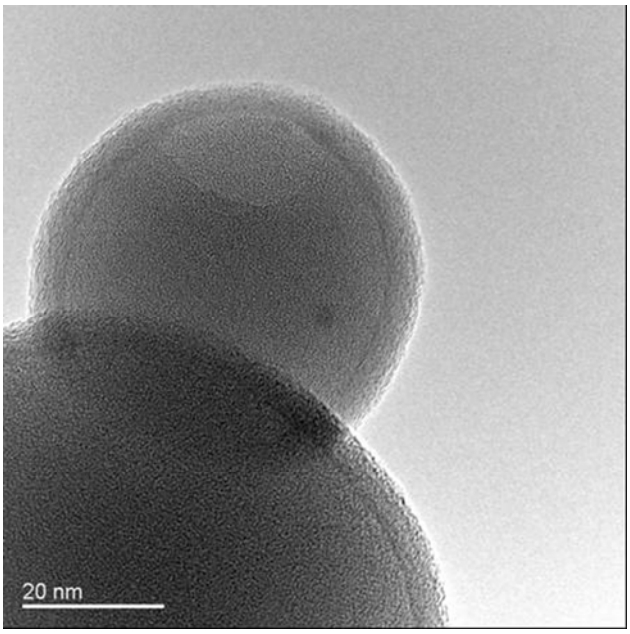

Figure 2. Transmission electron micrograph of alumina-coated silica nanoparticles after 50 coating cycles.

The TEM micrograph shows extremely conformal and uniform films around primary nanoparticles. The contrast between the film and the particle substrate is given by the difference in density between alumina and silica. For alumina ALD films, the density has been determined to be approximately 3.5 g/cm^3 [21] whereas the skeletal density of the primary silica particles is about 2.2 g/cm^3. The distinction between films deposited on different particles is also clear since no sintering between particles is observed. Even though aggregation of particles may occur, the interactions would be physical in nature and not due to the coating process.

The homogeneity of the deposited alumina films was studied using high-resolution microscopy analysis and Energy Dispersive Spectroscopy (EDS). This analysis performed a scan of the surface of coated nanoparticles generating a map of the signal of aluminum atoms on the particle substrate. A Hitachi S-5200 Field Emission Scanning Electron Microscope (FESEM) was used for this purpose. This equipment was coupled with a Princeton Gamma Tech Spirit Energy Dispersive Spectrometer (EDS) with a Li doped Si detector. The EDS analysis was performed at 15 kV.

An FESEM image is shown in Figure 3(a) and its corresponding aluminum-EDS signal in Figure 3(b). Due to strong London-Van der Waals forces, primary nanoparticles usually aggregate. The aluminum-EDS signal matches precisely the shape of this aggregate. This shows that the film deposited is homogenous throughout the particles forming the aggregate. Blank spaces within the EDS map correspond to voids within the aggregate of nanoparticles. Figure 3(a) is a 2-D representation of the aggregate, therefore only the outside coating can be detected. The conformality of the coating on single particles is proven by the TEM analysis. The non-granular nature of ALD films allows the uniform deposition of alumina on nanoparticles even under aggregating conditions.

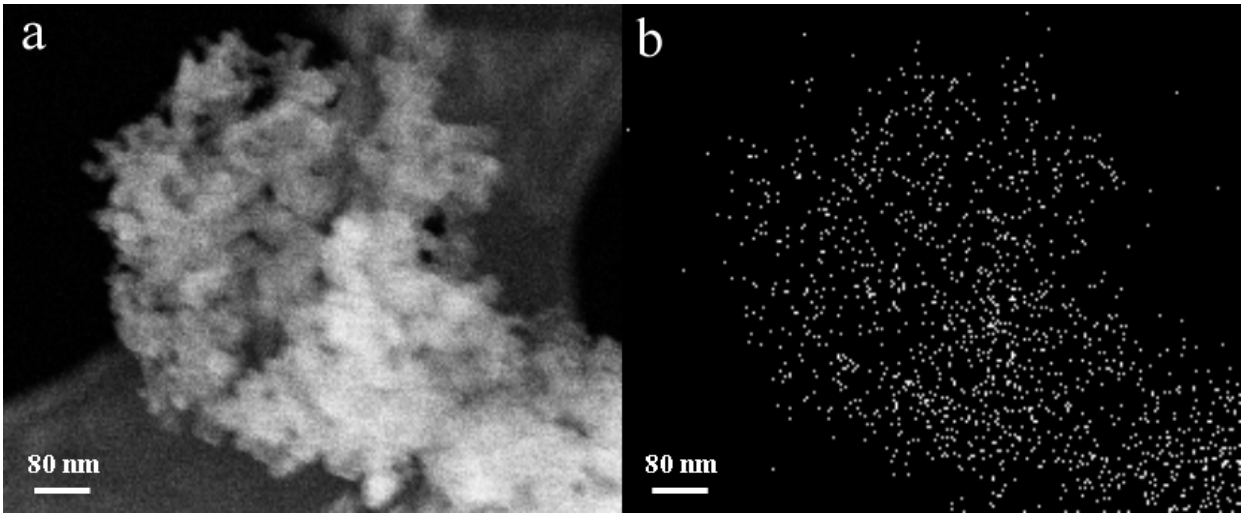

Figure 3 (a) and (b). FESEM image and aluminum-EDS signal for alumina-coated silica nanoparticles.

The composition of the particles after the coating process was analyzed using Fourier Transform Infrared Spectroscopy. A Nicolet 750 Magna-IR FTIR spectrometer was used for this analysis. The silica nanoparticles were supported by a tungsten grid obtained from Buckbee Mears. The tungsten grid (50.8 □m thick with 3.9 lines/mm) had dimensions of approximately 2 cm x 2 cm. The uncoated and alumina-coated silica nanoparticles were pressed into the grid using a manual press and polished stainless steel dies [22].

The vibrational mode of bulk alumina is located at a frequency of about 930 cm^{-1}. As observed in Figure 4, no features appear at this frequency for the uncoated silica sample. Al_2O_3 bulk vibrational modes appear for coated particles after 20 and 50 cycles. The frequency of the vibrational modes for the coated particles matches the one of A-16 SG alumina powder obtained from Alcoa Chemicals. This is a direct confirmation of the composition of the alumina films. The alumina spectrum for coated particles completely matches the one of the reference alumina powder and no features from the silica spectrum appear. This behavior is expected for conformally and uniformly coated particles [22].

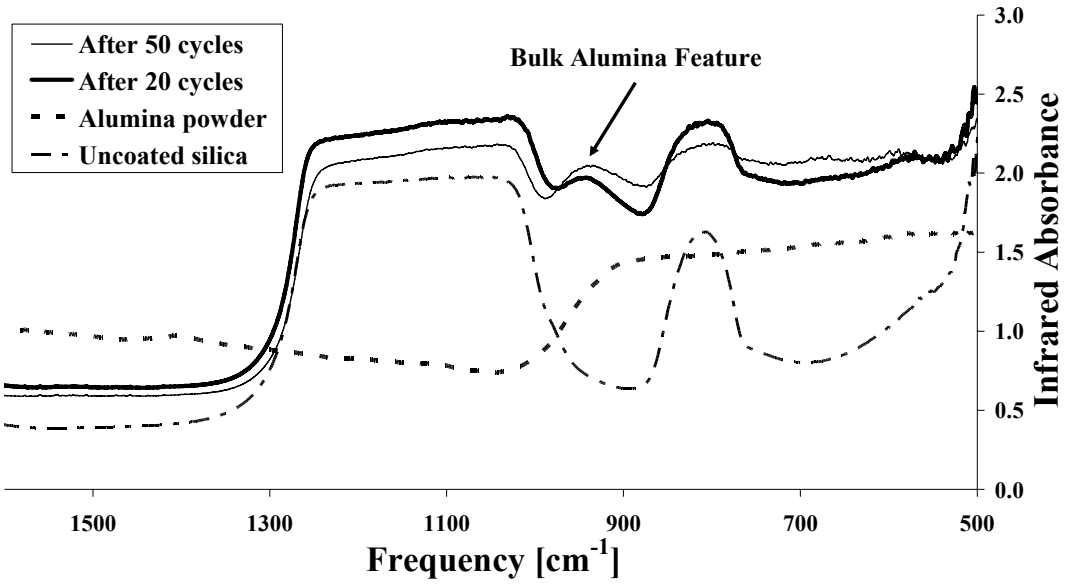

Figure 4. FTIR spectra of uncoated, reference alumina powder and alumina-coated silica nanoparticles after 20 and 50 cycles.

Conformality of the deposited alumina films was further tested by X-ray Photoelectron Spectroscopy as shown in Figure 5. A PHI 5600 Physical Electronics XPS with a high-energy resolution analyzer was used for this study. The analysis was performed using a magnesium source, pass energy of 58.7 eV and an energy step of 0.125 eV.

As shown in Figure 5, the highest-intensity peaks for SiO_2 (2p, 103.4 eV) and Si (2p, 99.15 eV) [28] have been completely attenuated as expected for a conformal film. Oxygen and aluminum features derive from the alumina film deposited on the nanoparticles. A tungsten grid, identical to the one used for FTIR studies, was used in this analysis to provide support for the particles. Tungsten features observed in the spectrum originate from this grid and carbon features correspond to background surface carbon.

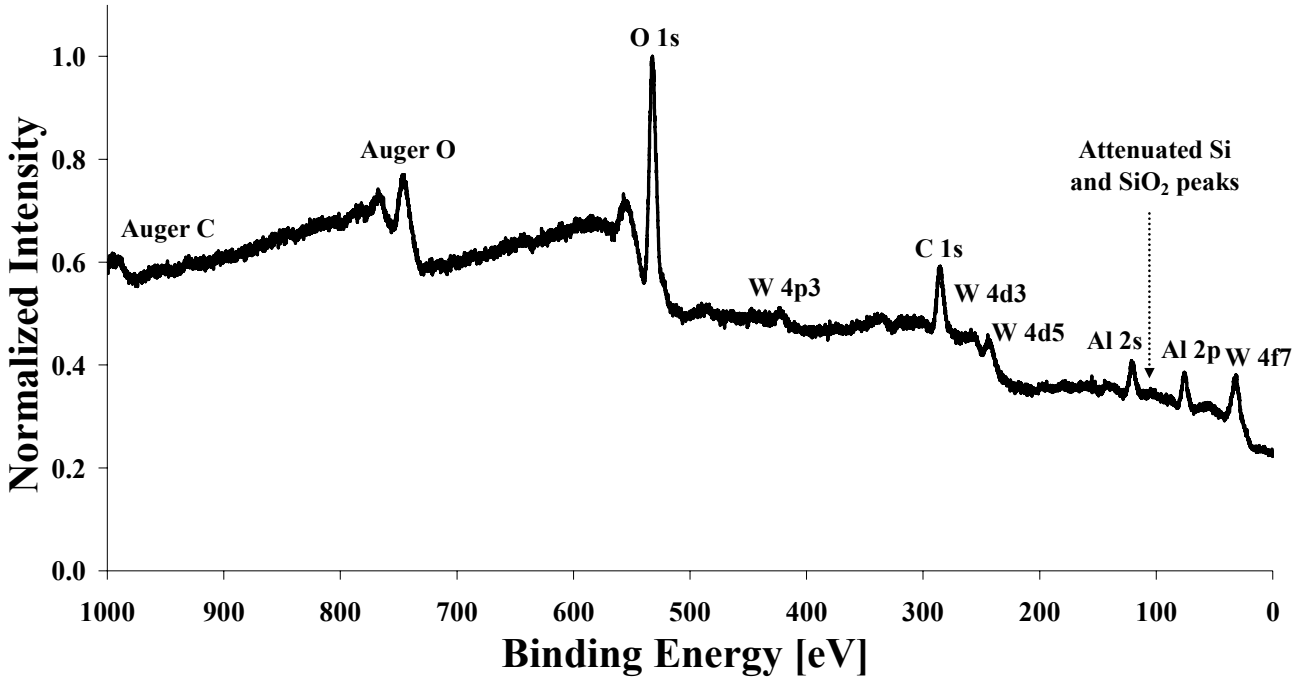

Figure 5. XPS spectrum of alumina-coated silica nanoparticles after 50 cycles.

2.3 Effect of coating on specific surface area

As studied by several researchers [25-27, 29], nanoparticles fluidize as aggregates of several hundreds of microns in size. If entire aggregates were coated, a drastic decrease in the specific surface area of the nanopowders would occur as ALD is capable of coating the narrow interstices inside the aggregates. Nonetheless, there is an expected change in the surface area of coated nanoparticles as the thickness of the film increases. This change occurs due to the slight increase in the particle diameter as well as the change in the effective density. The prediction in the change of specific surface area for three different sizes of silica nanoparticles as the thickness of the alumina film increases is shown in Figure 6.

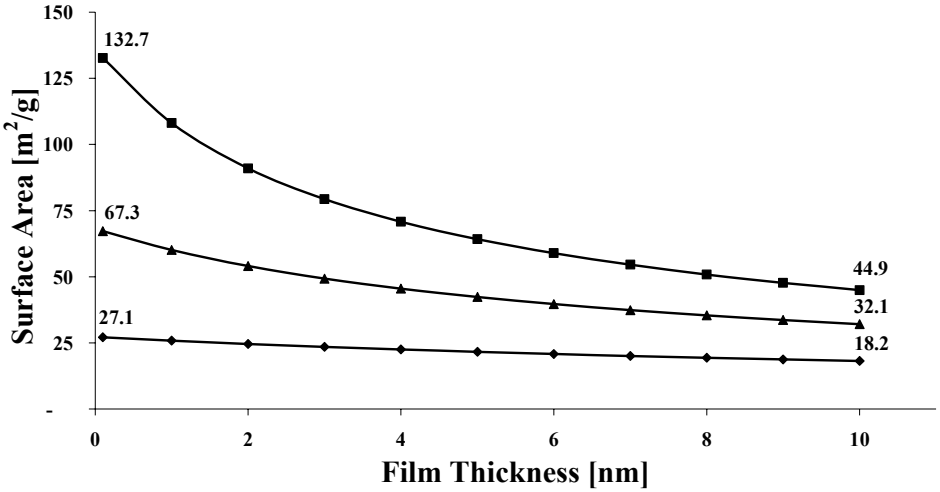

Figure 6. Prediction of change in specific surface area with increasing film thickness for different primary particle sizes. 20nm (■), 40 nm (▲), 100 nm (◆).

The surface area of silica nanoparticles was measured before and after 20 coating cycles using a Quantachrome Autosorb®-1. The experimental surface areas for uncoated and coated samples are 35.0 ± 3.9 and 29.6 ± 0.7 respectively. The prediction mentioned above, shows an expected change of 19.6% in the surface area after 20 cycles. The experimental change is 15.4%, lower that the predicted value, showing that nanoparticles are not being bonded together during the coating process.

The prediction shown in Figure 6 assumes spherical particles. However, the TEM micrograph shown in Figures 8 demonstrates that silica nanoparticles are not perfectly spherical. This is explained by the sintering process that occurs during the aerosol manufacturing of nanoparticles. Deviations from the predicted change in surface area can be attributed to this pre-coating condition.

3. Discussion

One of the main obstacles that different coating techniques have faced in trying to coat nanoparticles is their natural tendency for aggregation. As studied in the past, these aggregates are held together by a combination of interparticle forces [27].

Among several factors, aggregation of cohesive particles is dependent on flow conditions as well as the external energy that is transferred to particles during processing. Therefore, nanoparticles in different reactor configurations will show diverse aggregation patterns. Processing ALD coating of nanoparticles in a fluidized bed offers an advantage over other reactor designs. Higher heat and mass transfer coefficients and easy scalability are only a few examples. Additionally, due to the superior level of solids mixing in a fluidized bed, a behavior called dynamic aggregation is observed during fluidization of nanoparticles. This unique characteristic observed in fluidized beds along with the self-limiting nature of ALD allows for conformally coated individual nanoparticles.

Due to constant solids recirculation and gas flow through a fluidized bed, dynamic aggregates partially break apart and reform during fluidization. In this process, outer edges of fluidizing aggregates are shed and picked up by other aggregates. Even though this breakage is partial, due to continuous recirculation and frequent collisions, the entire surface of all the particles will be exposed to the fluidizing gas in very short times. If the same gas precursor atmosphere is kept during this time (the time it takes to expose the entire surface of all particles) the surface will be completely saturated and individual nanoparticles can be coated.

The adsorption of gas phase precursors on the surface of nanoparticles may occur by means of two competing mechanisms. On one hand, dynamic aggregation allows for exposing the entire surface of particles if processed for long enough times. On the other hand, the surface of individual nanoparticles can be reached by reactants that diffuse inside dynamic aggregates. The channels formed between individual nanoparticles within an aggregate are extremely narrow and the diffusion process would be very slow [30]. This implies that surface adsorption of gas precursors will predominantly take place during aggregate shearing.

Atomic Layer Deposition is the only known method capable of coating individual nanoparticles with carefully controlled conformal films. Sequential self-limiting chemical reactions take place on the particle surface and not in the gas phase. Other methods have intrinsic limitations to conformally coat individual nanoparticles while keeping control of the film thickness.

4. Conclusions

This work represents the first successful attempt to coat individual silica nanoparticles with ultrathin films that are highly conformal and uniform in thickness at a large scale using ALD. A fluidized bed reactor allowed the processing of bulk quantities of nanopowders using ALD. The composition of the alumina films was confirmed by Infrared Spectroscopy, X-ray Photoelectron Spectroscopy and Energy Dispersive Spectroscopy. Highly conformal and uniform films were observed via Transmission Electron Microscopy and Field Emission Scanning Electron Microscopy. The specific surface area of nanoparticles varied slightly as theoretically expected. Primary nanoparticles are coated individually due to their dynamic aggregation behavior during fluidization and the self-limiting characteristics of sequential surface reactions by ALD.

5. Experimental

Silica nanoparticles were coated using an ALD Fluidized Bed Reactor. A schematic of the experimental apparatus is shown in Figure 7. The reactor is a stainless steel column with a 20-□m pore size porous metal disc as the gas distributor. A porous stainless steel filter element (0.5 □m pore size) was used at the inside top of the reactor column to prevent particles from leaving the system.

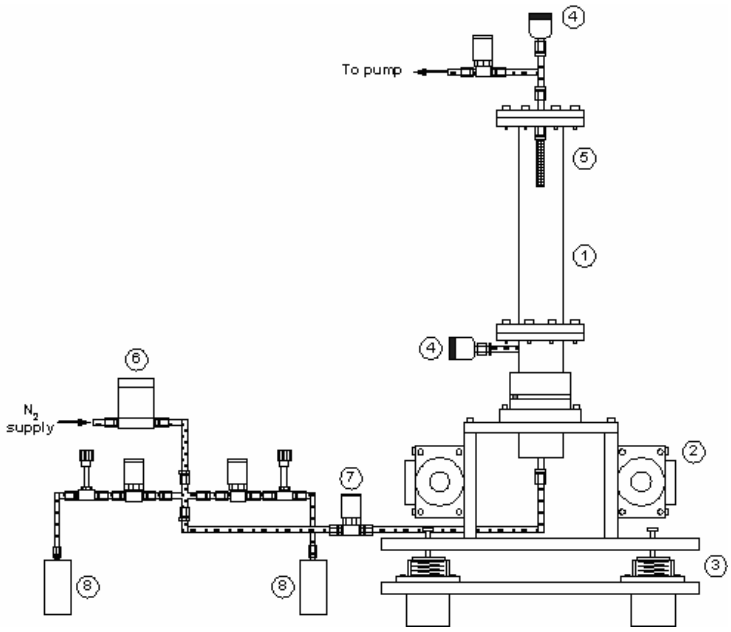

Figure 7. Schematic of ALD-FBR apparatus: 1) reaction column, 2) vibro-motors, 3) spring supports, 4) pressure transducers, 5) sintered-metal filter, 6) mass flow controller 7) pneumatic valve, 8) reactant containers.

The coating process was performed at reduced pressures and under mechanical vibration. Reduction of pressure in the column was achieved by controlling the opening of a diaphragm valve placed at the inlet of an Alcatel 2063 vacuum pump. Two synchronized vibro-motors from Martin Engineering were utilized to vibrate the column. A vibration frequency of 20 Hz and amplitude of 3.3 mm were used. Four spring supports on the platform gave homogeneous vertical vibration to the entire system.

High-purity nitrogen was used as the fluidizing gas. Its flowrate was controlled by an MKS® 1179 series mass flow controller. MKS® 902 series piezo transducers were located below the distributor plate and at the outlet of the fluidization column to measure the pressure drop across the bed of powder.

Aerosil OX-50™ silica nanoparticles were obtained from Degussa Corp. They were 40 nanometers in primary particle size and had a BET surface area of 50 ± 15 m^2/g. The bulk density of the powder was 130 kg/m^3 and the skeletal density of primary nanoparticles was approximately 2200 kg/m^3. Aggregation tendency and some sintering were observed in the uncoated sample as shown in Figure 8. Before loading, powders were sieved using a 40 mesh screen. Particles were then dried at 400 K and 0.5 Torr for 2 hours inside the reactor and under continuous flow of nitrogen.

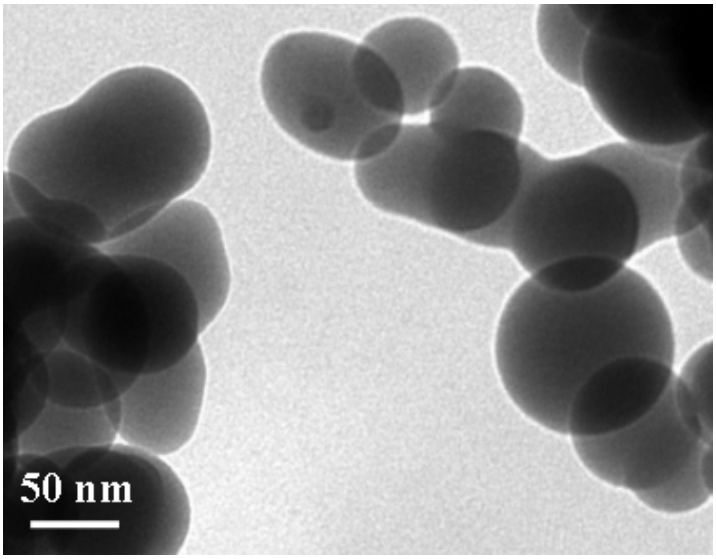

Figure 8. Transmission electron micrograph of uncoated silica nanoparticles

The fluidized bed reactor was encased by a clamshell-type furnace from Marshall Furnace Co. The reaction temperature was 450 K. The feeding lines were also heated to approximately 350 K. Trimethylaluminum obtained from Sigma-Aldrich and deionized water, were used as reactants. The reactants were fed via their vapor pressures and the system was kept at low pressure (~ 1 Torr).

During each coating cycle, the reactants were fed for enough time so saturation of all active sites occurred for every dose. This time was calculated based upon the surface area of the nanoparticles and the sample mass utilized for each batch. After each reactant dose, the system was flushed with inert gas to eliminate unreacted species as well as any methane formed during reaction.

Particle/Droplet Image Analysis (PDIA) using an Oxford Lasers VisiSizer^{TM} was used to investigate the aggregation of nanoparticles as they fluidized. The laser provided pulses of infrared light at a wavelength of 805 nm. The laser was coupled with a monochrome digital camera (Kodak Mega-Pixel Model ES1.0) using a standard silicon charge-coupled device sensor.

The laser and camera were triggered so that a single laser pulse froze the motion of the aggregates during each frame capture. The maximum analysis rate of the system was 30 frames per second. The pixel area of the particle aggregates was then measured and a special calibration of the system allowed the equivalent aggregate diameter to be calculated.

Acknowledgements
This work was funded by the National Science Foundation (Grant NER-0210670), the Department of Education GAANN Program in Functional Materials and the University of Colorado Engineering Excellence Fund.

The authors thank Jarod McCormick at the University of Colorado at Boulder for performing the XPS analysis as well as Geoff Courtin and William Kroenke at the Center for Micro-Engineered Materials at the University of New Mexico for performing the FESEM-EDS studies on coated nanoparticles.

References

[1] V.S. Nagarajan, S. Jahanmir, and V.P. Thompson, *Dental Materials*, **2004**. *20*(1): p. 63-71.
[2] N. Emami, M. Sjodahl, and K.-J.M. Soderholm, *Dental Materials*, **2005**. *21*(8): p. 721-730.
[3] J.P. Dan, H.J. Boving, and H.E. Hintermann, *Journal De Physique Iv*, **1993**. *3*(C7): p. 933-941.
[4] B. Hong, et al., *Diamond and Related Materials*, **1997**. *6*(1): p. 55-80.
[5] B.K. Kellerman, et al., *Surface Science*, **1997**. *375*(2-3): p. 331-339.
[6] M. Karches, M. Morstein, and P. Rudolf von Rohr, *Surface and Coatings Technology*, **2003**. *169-170*: p. 544-548.
[7] J. Kim, G.Y. Han, and C.-H. Chung, *Thin Solid Films*, **2002**. *409*(1): p. 58-65.
[8] I. Sanchez, et al., *Powder Technology*, **2001**. *120*(1-2): p. 134-140.
[9] H.S. Shin and D.G. Goodwin, *Materials Letters*, **1994**. *19*(3-4): p. 119-122.
[10] V.V. Srdic, et al., *Nanostructured Materials*, **1999**. *12*(1-4): p. 95-100.
[11] D. Vollath and D.V. Szabo, *Nanostructured Materials*, **1994**. *4*(8): p. 927-938.
[12] S.M. George, A.W. Ott, and J.W. Klaus, *J. Phys. Chem.*, **1996**. *100*(31): p. 13121-13131.
[13] C. Goodman and M. Pessa, *J. Appl. Phys.*, **1986**. *60*(3): p. R65-R81.
[14] T. Suntola, *Thin Solid Films*, **1992**. *216*(1): p. 84-89.
[15] A.C. Dillon, et al., *Surface Science*, **1995**. *322*(1-3): p. 230-242.
[16] J.F. Fan, K. Sugioka, and K. Toyoda, *Japanese Journal of Applied Physics Part 2-Letters*, **1991**. *30*(6B): p. 1139-1141.
[17] G.S. Higashi and C.G. Fleming, *Applied Physics Letters*, **1989**. *55*(19): p. 1963-1965.
[18] H. Kumagai and K. Toyoda, *Applied Surface Science*, **1994**. *82-83*: p. 481-486.
[19] M. Ritala, et al., *Thin Solid Films*, **1996**. *286*(1-2): p. 54-58.
[20] C. Soto and W.T. Tysoe, *Journal of Vaccum Science & Technology A*, **1991**. *9*(5): p. 2686-2695.
[21] A.W. Ott, et al., *Thin Solid Films*, **1997**. *292*: p. 135-144.
[22] J.D. Ferguson, A.W. Weimer, and S.M. George, *Applied Surface Science*, **2000**(162/163): p. 280-292.
[23] J.R. Wank, S.M. George, and A.W. Weimer, *Journal of the American Ceramic Society*, **2004**. *87*(4): p. 762-765.
[24] J.R. Wank, S.M. George, and A.W. Weimer, *Powder Technology*, **2004**. *142*(1): p. 59-69.
[25] C.H. Nam, R. Pfeffer, and R.N. Dave. in *Fluidization XI 11th International Conference on Fluidization*. **2004**. Naples, Italy: Engineering Conferences International.

[26] J.R. Wank, A.W. Weimer, and S.M. George, *Powder Technology*, **2001**. *121*(2-3): p. 195-204.
[27] W. Yao, et al., *Powder Technology*, **2002**. *124*(1-2): p. 152-159.
[28] C.D. Wagner, et al., *Handbook of X-Ray Photoelectron Spectroscopy*. **1979**, Eden Prairie, MN: Perkin-Elmer Corporation.
[29] S. Matsuda, H. Hatano, and A. Tsutsumi, *Chemical Engineering Journal*, **2001**. *82*(1-3): p. 183-188.
[30] P. Norberg, L.-G. Patersson, and I. Lundstrom, *Vacuum*, **1994**. *45*(1): p. 139-144.